JACS
JOURNAL OF THE AMERICAN CHEMICAL SOCIETY
Article
pubs.acs.org/JACS

Quantum Beats in Crystalline Tetracene Delayed Fluorescence Due to Triplet Pair Coherences Produced by Direct Singlet Fission

Jonathan J. Burdett and Christopher J. Bardeen*

Department of Chemistry, University of California, Riverside, 501 Big Springs Road, Riverside, California 92521, United States

Supporting Information

ABSTRACT: A detailed analysis of the oscillations seen in the delayed fluorescence of crystalline tetracene is presented in order to study the mechanism of singlet fission. Three quantum beat frequencies of 1.06 ± 0.05, 1.82 ± 0.05, and 2.92 ± 0.06 GHz are resolved, which are damped on a time scale of 20 ns. The effects of sample morphology, excitation wavelength, and temperature are examined. A density matrix model for singlet fission is developed that quantitatively describes the frequencies, amplitudes, and damping of the oscillations. The model assumes a direct coupling of the initially excited singlet exciton to the triplet pair manifold. There is no electronic coherence between the singlet and triplet pair states, but the rapid singlet decay time of ~200 ps in solution-grown single crystals provides the impulsive population transfer necessary to create a coherent superposition of three zero-field triplet pair states $|xx\rangle$, $|yy\rangle$, and $|zz\rangle$ with overall singlet character. This superposition of the three states gives rise to the three quantum beat frequencies seen in the experiment. Damping of the quantum beats results from both population exchange between triplet and singlet manifolds and pure dephasing between the triplet pair states. By lowering the temperature and slowing the SF rate, the visibility of the oscillations decreases. There is no evidence of magnetic dipole−dipole coupling between the product triplets. Our model provides good overall agreement with the data, supporting the conclusion that singlet fission in tetracene proceeds through the "direct" mechanism without strong electronic coupling between the singlet and triplet pair states.

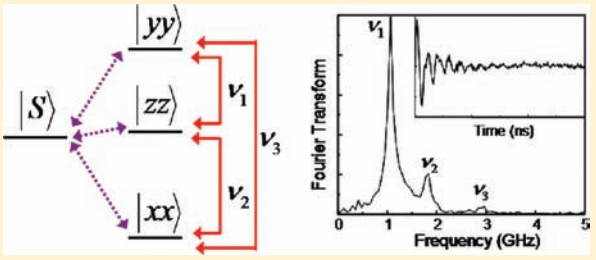

INTRODUCTION

Photovoltaic cells based on organic and inorganic semiconductors are a promising way to convert solar photons into electrical energy. In the pursuit of higher efficiency photovoltaic cells, new photophysical phenomena are being investigated. One of the most promising ways to surpass the Shockley−Quiesser limit for single junction photovoltaic cells is to convert the excess energy in above-the-gap photons into more than one electron−hole pair.[1,2] Multiple exciton generation in inorganic semiconductor nanocrystals is one example of how new types of materials could make this possible.[3,4] Although the mechanism and overall efficiency of this process is still debated, recent results indicate that it can lead to photocurrent yields in excess of 100%.[5,6] Multiple exciton generation has also been observed in carbon nanotubes,[7,8] and in molecular solids, an analogous phenomenon called singlet fission (SF) has been known for almost 50 years.[9,10] Unlike intersystem crossing, where a singlet state is converted into one triplet state via a spin flip, SF is a four-electron, spin-allowed process whereby an initially created singlet exciton spontaneously splits into a pair of triplet excitons. Conservation of energy requires that the energy of the triplet must be half that of the singlet, but theoretical surveys predict that large numbers of conjugated molecules could fulfill this requirement.[11] First observed in polyacene molecular crystals, SF has now been shown to occur in molecular aggregates and solid state thin films composed of a variety of conjugated molecules, with efficiencies approaching 200%.[12−15] Covalent dimers have also exhibited SF, although the efficiencies tend to be lower in these systems.[16−18] In order to design new materials that can lead to practical improvements in photovoltaic efficiencies, a better quantitative understanding of this phenomenon is needed. Recent theoretical work[19−22] has clarified the distinction between the "direct" mechanism of SF, where the multiple exciton state is produced in a single step, and the "indirect" mechanism where sequential electron transfer events require the involvement of an intermediate charge-transfer state.[10] It is an open question as to which mechanism is actually operative in a given molecular system.

Crystalline tetracene has long served as a prototypical SF material.[23] In previous work, the observation of the triplets formed by SF in tetracene has relied on the detection of electron spin resonance signals[24−27] and magnetic field effects on both fluorescence[28−30] and device performance.[31] Transient absorption experiments on crystalline tetracene and pentacene[32−36] have provided valuable information regarding the excited state dynamics, although the assignment of various spectral features can be complicated.[37−39] The indirect observation of triplet dynamics using the delayed fluorescence (DF) signal can also provide a wealth of valuable information about triplet dynamics, as illustrated by the work by Chabr et al.[40,41] Their observation of quantum beats in the DF signal

Received: February 20, 2012
Published: April 24, 2012

   dx.doi.org/10.1021/ja301683w | J. Am. Chem. Soc. 2012, 134, 8597−8607

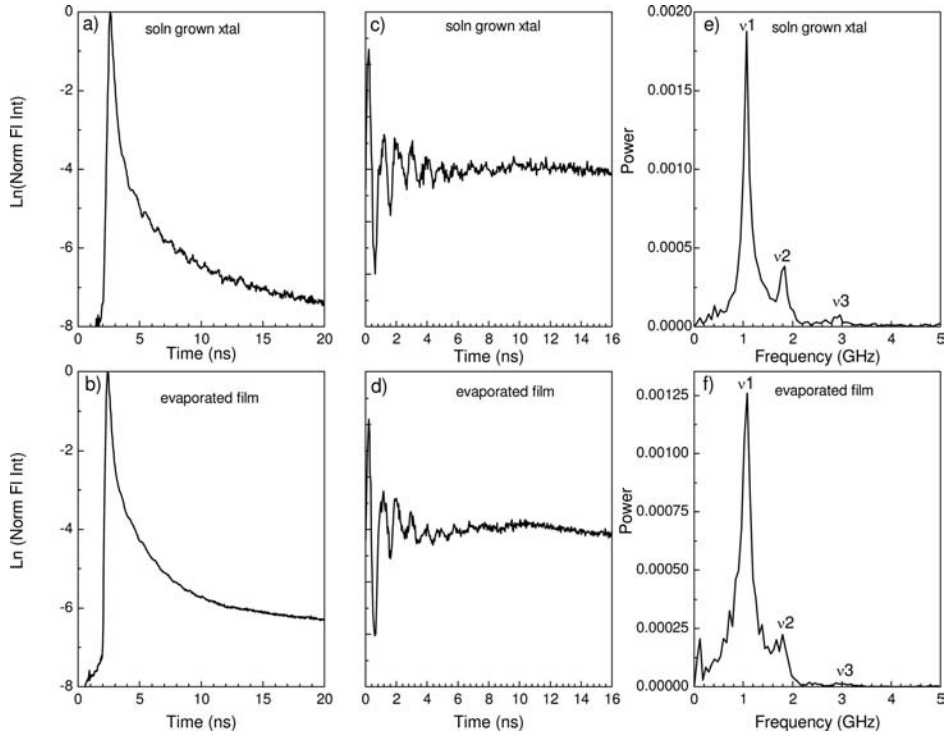

Figure 1. (a) Time-resolved fluorescence of a solution-grown single crystal of tetracene. (b) Time resolved fluorescence of a vacuum-evaporated polycrystalline tetracene film. (c) Oscillations extracted from the fluorescence decay of a solution-grown single crystal shown in panel a by subtracting off an exponential fit. (d) Oscillations extracted from the fluorescence decay of a vacuum-evaporated polycrystalline tetracene film shown in panel b by subtracting off an exponential fit. (e) The Fourier transform of the extracted oscillations of the single crystal from panel c with peaks at 1.06 ± 0.05, 1.83 ± 0.05, and 2.92 ± 0.06 GHz. (f) The Fourier transform of the extracted oscillations of the polycrystalline film from panel d with peaks at 1.08 ± 0.05, 1.80 ± 0.05, and 2.99 ± 0.08 GHz.

corresponding to the energy levels of the triplet pair provided direct proof of the formation of triplet pair superposition states through the SF process. Their work concentrated on the behavior of samples in high magnetic fields, and the relatively low signal-to-noise ratio made it difficult to reliably measure quantities like damping times. Also, a model that could quantitatively describe both the excitation and decoherence of the oscillations required a density matrix treatment, which was not performed. In the current paper, we revisit that work in an effort to clarify both the origin and the dynamics of the quantum beats observed in the DF in the absence of a magnetic field. We find that they are a general phenomenon, present in both single crystals and evaporated thin films, and that they exhibit a strong temperature dependence. We develop a hybrid coherent−incoherent density matrix model that involves the direct creation of a coherent superposition of triplet pair states via incoherent relaxation of the initially excited singlet state. This model does a good job of reproducing the overall fluorescence decay shape, the relative Fourier amplitudes of the oscillations, and their damping. It does not require the existence of an intermediate state or electronic coherence between the singlet and triplet manifolds. Lastly, our modeling indicates that magnetic dipole−dipole interactions between the two triplets created by SF are small. This suggests that the triplets either must reside on non-nearest neighbor molecules or are moving so rapidly that the dipole−dipole interaction is averaged to zero. The results in this paper help clarify the dynamics of SF in crystalline tetracene and provide a starting point for the development of more sophisticated models for this process.

EXPERIMENTAL SECTION

All tetracene samples were made using tetracene purchased from Aldrich (sold as benz[*b*]anthracene sublimed grade, 99.99% trace metals basis) and used as received. In order to prevent oxidation, the tetracene vial and all samples were kept in an evacuated desiccator in order to limit their exposure to oxygen. Single crystals of tetracene were formed on glass slides and coverslips by solvent evaporation from a saturated tetracene solution in toluene with a concentration of 7×10^{-4} M. Using this method, we could grow ultrathin (<100 nm) single crystals with areas of up to 1 mm^2. These thin crystals are necessary to prevent self-absorption distortions of the fluorescence spectrum. Single crystals were identified using polarizing microscopy with light >550 nm in order to minimize photoxidation. Polycrystalline films were grown by vacuum evaporation in a Pelco vacuum evaporator onto a glass microscope slide at pressures less than 1.5×10^{-5} Torr.

Time-resolved fluorescence experiments were conducted using front face detection with a Hamamatsu C4334 Streakscope picosecond streak camera. All measurements were taken with the crystals mounted inside of an evacuated cryostat with pressures of 1×10^{-3} Torr or less or under an argon atmosphere, achieved by gluing a coverslip to the glass slide with Torrseal epoxy. The 400 nm excitation was provided by frequency doubling the 800 nm output of a 40 kHz Spectra-Physics Spitfire Ti:sapphire regenerative amplifier in a BBO crystal. In order to prevent scattering of the 400 nm excitation light into the streak camera, a 450 nm long wave pass filter and a 420 nm color filter were placed before the streak camera. White light continuum generation in a 3 mm sapphire plate served as the source for 500 nm excitation, which was isolated with a 10 nm bandwidth interference filter. A 515 nm cutoff filter and 514 nm interference filter were used to prevent scattered excitation from reaching the streak camera. Since exciton−exciton annihilation has been found previously to be a problem in tetracene samples,[42−44] the fluences in these experiments was kept at 6×10^{-6} J cm^{-2} or less, well below the threshold for exciton−exciton

dx.doi.org/10.1021/ja301683w | J. Am. Chem. Soc. 2012, 134, 8597−8607

annihilation. Lowering the fluence below this level did not change the oscillation frequencies or visibility.

The appearance of the oscillations did not depend on the orientation of the single crystal relative to the excitation light polarization or the detection. In order to isolate the oscillations on top of the background decay, the fluorescence decay was fit with either a double or triple exponential with an offset. This fit was then subtracted from the decay, leaving the oscillations centered on zero, with between 390 and 450 time pixels. Fourier transforms were performed in Matlab using the built-in fast Fourier transform function. Simulated oscillation data was created by analytically solving the theoretical model described below with tetracene's parameters and varying the rates to achieve the best agreement with the experimental data. In order to accurately compare the simulated data with experiment, it was convolved with the instrument response along with adding an offset to account for the delayed fluorescence. The simulated data was 1001 points long, and the Fourier transforms were conducted on the simulated data with zero-filling out to 1024 points using the fast Fourier transform function in Matlab.

RESULTS

1. DF Oscillations in Single Crystals and Thin Films. Figure 1a,b shows the log plots of the fluorescence decays for both an ultrathin solution-grown single crystal and a polycrystalline thin film grown by vacuum evaporation. Both samples clearly exhibit ripples in the DF signal, although they are more pronounced in the single crystal data. In general, the visibility of the oscillations showed some variability from sample to sample, with the single crystals consistently showing higher visibility oscillations. When the fluorescence background is fit to a multiexponential and subtracted from the raw data, we can isolate the oscillatory component of the signal, as shown in Figure 1c,d. Both types of samples show similar frequencies and damping times. This can be seen most clearly from the Fourier power spectra of the data, which are shown in Figure 1e,f. In the spectrum of the single crystal in Figure 1e, we can discern three frequencies, which we denote $\nu_1 = 1.06 \pm 0.05$ GHz, $\nu_2 = 1.82 \pm 0.05$ GHz, and $\nu_3 = 2.92 \pm 0.06$ GHz. The noisier spectrum of the film in Figure 1f clearly shows ν_1, but the limited signal-to-noise makes it more difficult to discern features at ν_2 and ν_3. These three characteristic frequencies, ν_1, ν_2, and ν_3, were observed with the same relative amplitudes for all samples studied, although the overall oscillation visibility varied between samples. The same oscillations were observed in the DF using excitation at either 400 or 500 nm at room temperature. This lack of sensitivity to excess excitation energy is consistent with our previous results on the fluorescence decay dynamics of these samples.[42]

2. Simulation of DF Dynamics Using Density Matrix Approach. In order to quantitatively understand the origin of the dynamics seen in Figure 1, we first develop a model based on the density matrix description. In accordance with previous workers, we assume that the initially excited singlet state directly couples to the nine-state basis of triplet pair states. This is shown schematically in Figure 2. We use the zero-field basis, where $|x\rangle_A$, $|y\rangle_A$, and $|z\rangle_A$ are the eigenstates for the zero-field Hamiltonian (see Supporting Information for details) for an isolated triplet on site A.[45] The initially excited electronic state is in a singlet spin state, denoted $|S\rangle_{singlet}$. SF is a spin-allowed process because a superposition of triplet pair states can also have overall singlet character,[46,47] and in the zero-field basis, this superposition is given by

$$|S\rangle_{triplet} = \frac{1}{\sqrt{3}}(|xx\rangle + |yy\rangle + |zz\rangle) \quad (1)$$

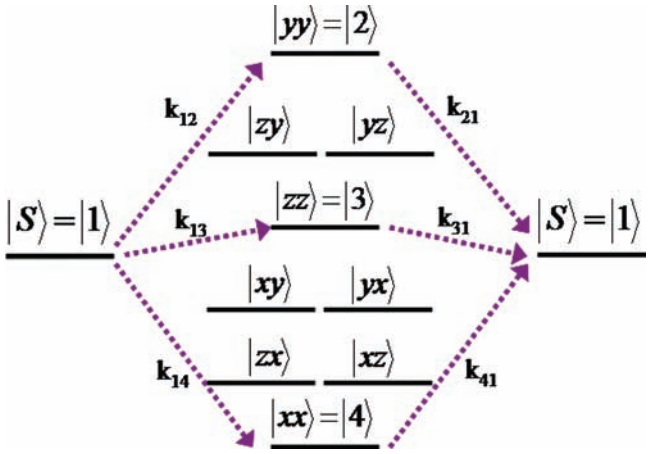

Figure 2. Schematic diagram illustrating the fission (k_{1n}) and fusion (k_{n1}) between the singlet state and the nine triplet pair states, which is the basis of the density matrix treatment described in the text.

The assumption underlying all spin-based theories of SF is that $|S\rangle_{singlet}$ maps directly onto $|S\rangle_{triplet}$. If this is the case, then the nonstationary triplet superposition state will evolve in time and give rise to quantum beats at frequencies corresponding to the energy differences between the $|xx\rangle$, $|yy\rangle$, and $|zz\rangle$ states. If the triplet pair state then couples back to the singlet at some later time t, we expect to see the singlet population be time-dependent, proportional to the overlap of $|S\rangle_{singlet}$ and $|S(t)\rangle_{triplet}$:[40]

$$\text{Recombined Singlet population} \propto |_{singlet}\langle S|S(t)\rangle_{triplet}|^2 \quad (2)$$

The frequencies of the quantum beats can be easily calculated. If there is no interaction between the triplets, the Hamiltonian is already diagonal in the zero-field basis and the stationary states are just the simple product states energies $|xx\rangle$, $|xy\rangle$, etc. The energies of the three states with singlet character, as deduced from eq 1, are

$$E_{xx} = 2E_x = 2\left(\frac{1}{3}D^* - E^*\right) \quad (3a)$$

$$E_{yy} = 2E_y = 2\left(\frac{1}{3}D^* + E^*\right) \quad (3b)$$

$$E_{zz} = 2E_z = 2\left(-\frac{2}{3}D^*\right) \quad (3c)$$

where D^* and E^* are the zero-field parameters for the crystal that can be obtained from EPR measurements.[24] The three possible energy differences, $xx - yy$, $xx - zz$, and $yy - zz$, provide the possible quantum beat frequencies. Using $D^* = -0.0062$ cm^{-1} and $E^* = 0.0248$ cm^{-1}, we find

$$E_{xx} - E_{yy} = 0.0992 \text{ cm}^{-1} = 2.98 \text{ GHz} \quad (4a)$$

$$E_{xx} - E_{zz} = 0.0620 \text{ cm}^{-1} = 1.86 \text{ GHz} \quad (4b)$$

$$E_{yy} - E_{zz} = 0.0372 \text{ cm}^{-1} = 1.12 \text{ GHz} \quad (4c)$$

The calculated difference frequencies given in eqs 4a−4c are all slightly higher than the frequencies extracted from the experimental Fourier transforms, but the close correspondence suggests that this analysis is on the right track. We should emphasize that this quantum beating results from recombina-

dx.doi.org/10.1021/ja301683w | J. Am. Chem. Soc. 2012, 134, 8597−8607

tion of coherent geminate triplet pairs and not from incoherent encounters between independently created triplets.

While a simple analysis of the state energies allows us to predict the quantum beat frequencies, a full density matrix treatment is required to understand the relative amplitudes and damping of the oscillations. A detailed derivation of the kinetic equations can be found in the Supporting Information, and below we outline our approach. In principle, such an analysis must describe the dynamics of the 10 coupled states (9 triplet pair plus 1 singlet). The simplifying assumption in all theories of SF and DF is that the transition rate from the singlet to the triplet manifold is proportional to the overlap of the triplet pair states and the wave function given in eq 1. Thus we can assume that only the triplet pair states with singlet character can participate in the SF/DF process. Typically there are only three such states, which we denote as 2, 3, and 4 with the singlet state denoted as state 1. We then write a Hamiltonian that includes an explicit coupling between state 1 (corresponding to $|S\rangle_{\text{singlet}}$) and states 2−4 (corresponding to $|xx\rangle$, $|yy\rangle$, and $|zz\rangle$ in the absence of the triplet−triplet interaction terms):

$$\hat{H} = \sum_{n=2}^{4} |n\rangle\varepsilon_n\langle n| + |n\rangle M_{n1}\langle 1| + |1\rangle M_{1n}\langle n| \tag{5}$$

The energy of the initial singlet state, $|1\rangle$, is set to 0, and the M_{1n} elements represent transition matrix elements that couple this state to the triplet pair states. In the following, we will assume that the M_{1n}'s are real numbers, that is, $M_{1n} = M_{n1}$. Setting $\hbar = 1$ and solving the Liouville equation with this Hamiltonian gives rise to first-order differential equations of the form

$$i\frac{\partial\rho_{11}}{\partial t} = \sum_{n=2}^{4} M_{1n}\rho_{n1} - \sum_{n=2}^{4} M_{n1}\rho_{1n} - \frac{i}{T_{\text{rad}}}\rho_{11} \tag{6a}$$

$$i\frac{\partial\rho_{1n}}{\partial t} = \sum_{k=2}^{4} M_{1k}\rho_{kn} - \varepsilon_n\rho_{1n} - M_{1n}\rho_{11} - \frac{i}{T_{2\text{TS}}}\rho_{1n} \tag{6b}$$

$$i\frac{\partial\rho_{nn}}{\partial t} = M_{n1}\rho_{1n} - M_{1n}\rho_{n1} - \frac{i}{T_{\text{trip}}}\rho_{nn} \tag{6c}$$

$$i\frac{\partial\rho_{nm}}{\partial t} = (\varepsilon_n - \varepsilon_m)\rho_{nm} + M_{n1}\rho_{1m} - M_{1m}\rho_{n1} - \frac{i}{T_{2\text{TT}}}\rho_{nm} \tag{6d}$$

Equations 6a−6d give the relevant terms: ρ_{11} represents the population in singlet state $|1\rangle$, ρ_{nn} represents the population in triplet pair state $|n\rangle$, and ρ_{1n} and ρ_{nm} represent coherences between $|1\rangle$ and $|n\rangle$ and $|n\rangle$ and $|m\rangle$ states, respectively. Note that in eqs 6a−6d, we have added four phenomenological relaxation rates: T_{trip} is the population relaxation time out of the triplet pair state that does not go back to the singlet; T_{rad} is the radiative lifetime of the singlet state, $T_{2\text{TS}}$ describes the electronic dephasing between the states in the triplet manifold and the singlet state, and $T_{2\text{TT}}$ describes the dephasing between triplet pair states. Consideration of all four states leads to a system of 16 coupled differential equations. The situation can be simplified somewhat if we assume that the singlet−triplet dephasing time, $T_{2\text{TS}}$, is much shorter than any other time scale in the problem. In this case, we can explicitly write the solution of the off-diagonal coherence terms between singlet and triplet states as

$$\rho_{1n}(t) = \int_{-\infty}^{t} \mathrm{d}t' \exp\left[\left(i\varepsilon_n - \frac{1}{T_{2\text{TS}}}\right)(t - t')\right] i\left(M_{1n}\rho_{11}(t') - \sum_{k=2}^{4} M_{1k}\rho_{kn}(t')\right) \tag{7}$$

As $T_{2\text{TS}}$ becomes very small, the exponential term can be approximated by a delta function, and we find that

$$\rho_{1n}(t) = iT_{2\text{TS}}\left(M_{1n}\rho_{11}(t) - \sum_{k=2}^{4} M_{1k}\rho_{kn}(t)\right) \tag{8}$$

The technique of letting $T_{2\text{TS}} \to 0$ to eliminate electronic coherences has been used previously to generate rate equations from the density matrix to describe rate processes in optical processes.[48,49] Physically, it means that the electronic coherences follow the population differences exactly and go immediately to zero in the absence of such a difference. Note that by taking this limit of rapid electronic dephasing between the singlet and triplet manifolds, we are considering SF to be an incoherent process with respect to the singlet → triplet transition. If the $T_{2\text{TS}}$ dephasing time were not much shorter than the other relevant time scales, then coherent coupling between the triplet and singlet manifolds would have at least two noticeable effects. First, the energy levels of both states would be shifted, similar to what is observed for excitonic coupling between states. Second the coherent nature of the population transfer would lead to Rabi-type oscillations of the population during times shorter than $T_{2\text{TS}}$. Although we see no sign of either phenomenon in tetracene, in pentacene recent time-resolved photoemission experiments have indicated the existence of an electronic coherence between the singlet and a multiple exciton state.[50] But it should be emphasized that our incoherent rate process can still generate electronic coherences between the triplet pair states. This type of phenomenon, where rapid electronic relaxation processes generate spin coherences, has been observed previously for both intersystem crossing and chemically reactive systems.[51−54] The validity of this approximation can be judged by whether the resulting calculations provide an accurate description of the data. We plug this new expression for ρ_{12}(t) back into the other differential equations for ρ_{11} and ρ_{nm} in order to obtain a new system of 10 coupled differential equations:

$$\frac{\partial\rho_{11}}{\partial t} = -\frac{1}{T_{\text{rad}}}\rho_{11} - \sum_{n=2}^{4} k_{1n}\rho_{11} + \sum_{n=2}^{4} k_{1n}\rho_{nn} + \sum_{n=2}^{4}\sum_{k\neq n,1}^{4} \frac{1}{2}\sqrt{k_{1n}k_{1k}}(\rho_{nk} + \rho_{kn}) \tag{9a}$$

$$\frac{\partial\rho_{nn}}{\partial t} = -\frac{1}{T_{\text{trip}}}\rho_{nn} + k_{1n}\rho_{11} - k_{1n}\rho_{nn} - \sum_{k\neq n,1}^{4} \frac{1}{2}\sqrt{k_{1n}k_{1k}}(\rho_{nk} + \rho_{kn}) \tag{9b}$$

$$\frac{\partial\rho_{nm}}{\partial t} = -\frac{1}{T_{2\text{TT}}}\rho_{nm} + i(\varepsilon_m - \varepsilon_n)\rho_{nm} + \sqrt{k_{1n}k_{1m}}\rho_{11} - \sum_{k=2}^{4} \frac{1}{2}\sqrt{k_{1m}k_{1k}}\rho_{nk} - \sum_{k=2}^{4} \frac{1}{2}\sqrt{k_{n1}k_{1k}}\rho_{km} \tag{9c}$$

dx.doi.org/10.1021/ja301683w | J. Am. Chem. Soc. 2012, 134, 8597−8607

where the population transfer rates, k_{1n}, are given by

$$k_{12} = 2T_{2TS}M_{12}^{\ 2} \tag{10a}$$

$$k_{13} = 2T_{2TS}M_{13}^{\ 2} \tag{10b}$$

$$k_{14} = 2T_{2TS}M_{14}^{\ 2} \tag{10c}$$

From a physical standpoint, the problem with eqs 9a−9c is that the rate of transfer forward (fission) is equal to the rate of transfer backward (fusion), which is not consistent with our physical observations. To fix this problem, we make an *ad hoc* assumption that the population decay rates from $1 \rightarrow n$ and $n \rightarrow 1$ are not equal. Furthermore, we assume that the population dephasing of the ρ_{nm} terms arises only from population loss, rather than gain. We now have

$$\frac{\partial \rho_{11}}{\partial t} = -\frac{1}{T_{rad}}\rho_{11} - \sum_{n=2}^{4} k_{1n}\rho_{11} + \sum_{n=2}^{4} k_{n1}\rho_{nn} + \sum_{n=2}^{4}\sum_{k\neq n,1}^{4} \frac{1}{2}\sqrt{k_{n1}k_{k1}}(\rho_{nk} + \rho_{kn}) \tag{11a}$$

$$\frac{\partial \rho_{nn}}{\partial t} = -\frac{1}{T_{trip}}\rho_{nn} + k_{1n}\rho_{11} - k_{n1}\rho_{nn} - \sum_{k\neq n,1}^{4} \frac{1}{2}\sqrt{k_{n1}k_{k1}}(\rho_{nk} + \rho_{kn}) \tag{11b}$$

$$\frac{\partial \rho_{nm}}{\partial t} = -\left(\frac{1}{T_{2TT}} + \frac{k_{m1}}{2} + \frac{k_{m1}}{2}\right)\rho_{nm} + i(\varepsilon_m - \varepsilon_n)\rho_{nm} + \sqrt{k_{1n}k_{1m}}\rho_{11} - \frac{1}{2}\sqrt{k_{m1}k_{n1}}(\rho_{nn} + \rho_{mm}) - \frac{1}{2}\sqrt{k_{m1}k_{l1}}\rho_{nl} - \frac{1}{2}\sqrt{k_{n1}k_{l1}}\rho_{lm} \tag{11c}$$

Note that the only difference between eqs 9a−9c and eqs 11a−11c is the change in subscripts on the rate constants for population transfer into versus out of a given state, that is, $k_{1n} \neq k_{n1}$. We can now solve this system of equations given the initial conditions $\rho_{11}(t = 0) = 1$ and $\rho_{nm}(t = 0) = 0$. The time evolution of the singlet state population $\rho_{11}(t)$ should be reflected in the time-dependent fluorescence, which is the experimental observable. For our simulations, the energy differences, ε_{nm}, are given by the energy differences between triplet pair energy levels, as obtained from either the unperturbed zero-field Hamiltonian (eqs 3) or by diagonalization of the Hamiltonian given in eqs 12−14 in section 5.

Although eqs 11a−11c contain multiple rates as free parameters, the data analysis allows us to fix them with reasonable accuracy. The radiative decay rate of the singlet exciton is fixed by our previous measurements on superradiant tetracene thin films to be $k_{rad} = 0.08\ ns^{-1}$, about twice that of molecular tetracene.[55] The initial decay of the singlet state is dominated by the sum of the k_{1n} rates, and for the single crystal, we found the prompt fluorescence decay time to be 202 ps. Then we have $k_{12} = k_{13} = k_{14} = 1/3 \times 1/0.202\ ns = 1.65\ ns^{-1}$, assuming equal transition probabilities to the three triplet pair states with singlet character. We note that this initial singlet decay time is significantly longer than what was observed in our previous experiments on polycrystalline evaporated thin films[42] but is within the range of what previous workers have observed in single-crystal tetracene samples.[44,56−58] The triplet fusion rates back to the singlet state determine the level of the DF signal relative to the peak of the prompt fluorescence signal (larger k_{n1} values lead to greater DF). We find that $k_{n1} = 0.1\ ns^{-1}$ gives a DF level close to what is observed experimentally. Note that in our model, these k_{n1} rates also contribute to the dephasing of the triplet pair state coherences and thus lead to damping of the oscillations. But we found that $k_{n1} = 0.1\ ns^{-1}$ was insufficient to account for all the damping, and we added a $T_{2TT} = 10$ ns in order to adequately reproduce the data. Last, we set the triplet population relaxation term $k_{trip} = 0.4\ ns^{-1}$ in order to describe the rapid initial decay of the SF seen in the 20 ns time window. The use of single k_{trip} value to describe the DF decay in the 2−20 ns time regime is clearly not sufficient, and it is likely that triplet diffusion and recombination lead to nonexponential kinetics. Nevertheless, this k_{trip} value is similar to that used to describe the intermediate time fluorescence decay in our previous experiments on tetracene thin films[42] and provides a way to parametrize our data.

In Figure 3a, we compare a simulation of the entire fluorescence signal, from the rising edge to the DF over 20 ns, with the experimental data. The parameters used in our

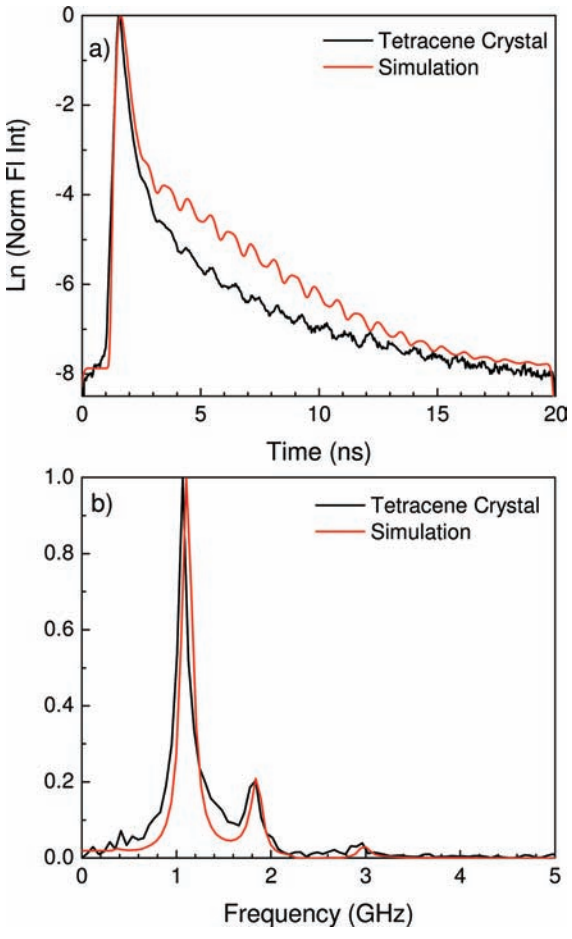

Figure 3. (a) Time-resolved fluorescence of a solution-grown single crystal of tetracene (black) along with simulated data convolved with an instrument response (red), where $k_{1n} = 1.65\ ns^{-1}$, $k_{n1} = 0.1\ ns^{-1}$, $k_{rad} = 0.08\ ns^{-1}$, $T_{2TT} = 10$ ns, $k_{trip} = 0.4\ ns^{-1}$, $D^* = -0.186\ ns^{-1}$ and $E^* = 0.744\ ns^{-1}$. (b) Normalized Fourier transforms of the extracted frequencies from solution-grown single crystal of tetracene (black) along with simulated data convolved with an instrument response (red) with the same parameters as panel a.

dx.doi.org/10.1021/ja301683w | J. Am. Chem. Soc. 2012, 134, 8597−8607

simulation, along with brief descriptions of how they were determined, are provided in Table 1. For the simulation, we

Table 1. Simulation Parameters and Origin of Values

$k_{12} = k_{13} = k_{14} = (1/3)k_{fiss} = 1.65\ ns^{-1}$	k_{fiss} was fixed from exponential fits to the initial fluorescence decay over the first 300 ps
$k_{n1} = 0.1\ ns^{-1}$	k_{n1} was varied in order to best fit the level of delayed fluorescence
$T_{2TT} = 10$ ns	T_{2TT} was varied in order to best fit the oscillation damping
$k_{trip} = 0.4\ ns^{-1}$	k_{trip} was varied in order to best fit the delayed fluorescence decay
$k_{rad} = 0.08\ ns^{-1}$	k_{rad} was fixed based on previous fluorescence experiments[55]
$D^* = -0.186\ ns^{-1}$	D^* was fixed based on EPR measurements[24]
$E^* = 0.744\ ns^{-1}$	E^* was fixed based on EPR measurements[24]

convolved the calculated decay with a 15 ps full-width-half-maximum instrument response. The simulated data does a decent job of reproducing the overall signal shape as well as the amplitude and damping of the oscillations for the single crystal. These calculated oscillations are significantly larger than those observed in an evaporated film, as shown in Figure 1. This suggests that sample preparation plays a role in determining the oscillation visibility. We suspect that structural disorder in the polycrystalline film leads to some fraction of the triplet pairs that undergo dephasing of their spin states very rapidly. Triplet pairs that have collapsed into their constituent $|xx\rangle$, $|yy\rangle$, and $|zz\rangle$ pair states can still undergo fusion and contribute to the DF signal, but such states will not lead to the quantum beats that are the signature of the superposition states. A second point is that the FT peaks in Figure 5b from the simulation data using the energy difference given in eqs 3a−3c are all shifted slightly to lower frequency due to the strong damping. Taking into account the error ranges in the D^* and E^* values obtained by Yarmus et al.,[24] the FT peaks in the simulations are calculated to appear at frequencies ranging from 1.07 to 1.17 GHz, 1.76 to 1.90 GHz, and 2.88 to 3.03 GHz. All three of these frequency ranges fall within the error range of our experimentally measured frequencies. Thus our measurements agree with those predicted by the zero-field Hamiltonian for a single triplet exciton to within the experimental error. Finally, we note that the oscillations in the data and simulation move out of phase over the 20 ns time window. This discrepancy most likely results from the sensitivity of the absolute phase of the oscillations to the overall decay shape, which is not correctly captured by our simple exponential decay, as noted in the previous paragraph.

3. Dependence of Oscillations on SF Rate. The relative amplitudes of the three beat frequencies are quite sensitive to the SF rate as given by k_{1n}. To understand this phenomenon, we can consider two limits: very fast SF and very slow SF. In the limit of very rapid SF, the process acts like an ultrafast pulse that impulsively excites the triplet manifold, creating a narrow wavepacket that oscillates equally among the three states. Since all three triplet pair states have the same singlet projection, we would expect equal amplitude oscillations from all three possible coherences: *xx*−*yy*, *xx*−*zz*, and *yy*−*zz*. In the opposite limit of very slow SF, the population transfer is much slower than the oscillation frequency, and there is no opportunity to create a wavepacket. In this limit, no quantum beats would be observed. In Figure 4, we compare simulations for different k_{1n} rates, where the k_{n1} rates have been fixed to be 0.1 ns^{-1}. As

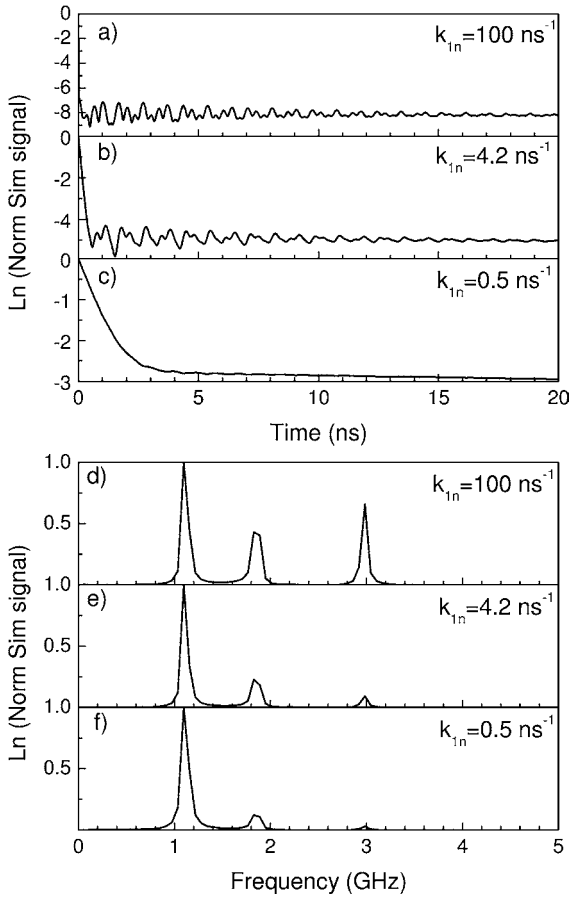

Figure 4. Simulated oscillations for k_{1n} = (a) 100 ns^{-1}, (b) 4.2 ns^{-1}, and (c) 0.5 ns^{-1} with k_{n1} = 0.1 ns^{-1}, T_{2TT} = 10 ns, $D^* = -0.186\ ns^{-1}$, and $E^* = 0.744\ ns^{-1}$. Normalized Fourier transforms of the simulated oscillations in panels a, b, and c are found in panels d, e, and f, respectively.

expected, very rapid SF rates lead to comparable amplitude oscillations at all three beat frequencies. As k_{1n} is decreased, not only do the overall amplitudes of all the oscillations decrease relative to the rest of the signal, as seen in Figure 4a−c, but in addition the amplitudes of the higher frequency oscillations decrease relative to the lowest frequency *yy*−*zz* oscillation. For $k_{1n} = 0.5\ ns^{-1}$, the highest frequency *xx*−*yy* oscillation peak is no longer visible. In order to obtain the FT profile observed experimentally, our k_{1n} rates must be in the intermediate regime, where the low-frequency *yy*−*zz* oscillation is efficiently excited, but the high-frequency *xx*−*yy* oscillation is barely excited. The data in Figure 3b show that the k_{1n} rates deduced from the decay rate of the prompt fluorescence are consistent with the Fourier amplitude analysis. In essence, two independent measurements, the FT amplitudes and the fluorescence decay rate, give the same SF rate. A second observation from our modeling is that the damping of the oscillations results from both k_{n1} population exchange between the singlet and triplet manifolds and from pure T_{2TT} dephasing between the triplet levels themselves. Thus the DF process that allows us to detect the triplets also destroys their spin coherence. In a system where the triplet fusion leading to DF is much slower or nonexistent, for example, crystalline pentacene, it may be possible that the triplet superposition state can persist for a longer time.

dx.doi.org/10.1021/ja301683w | J. Am. Chem. Soc. 2012, 134, 8597−8607

4. Temperature Dependence of Oscillations. The idea that changing the SF k_{1n} rates can change the visibility and relative amplitudes of the quantum beats can be tested by changing the temperature of the sample. Figure 5a–d shows the

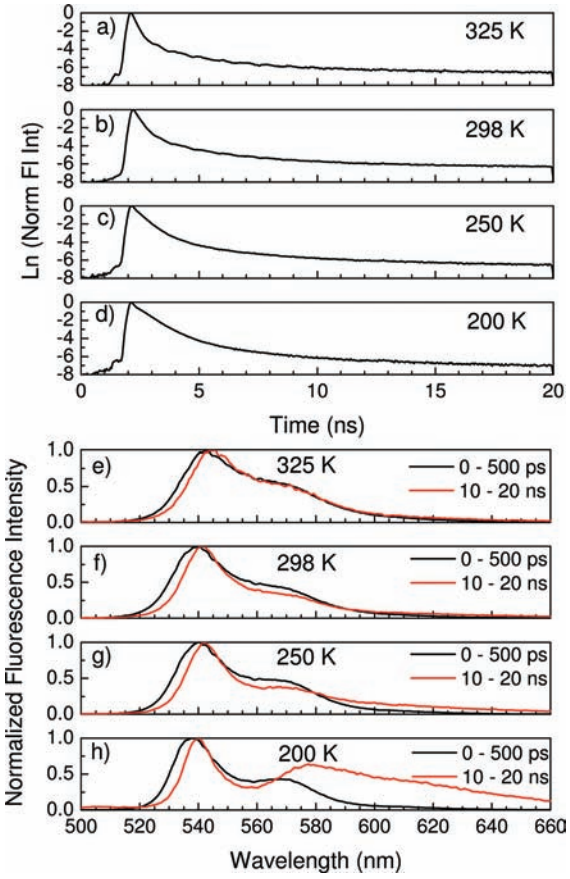

Figure 5. Time-resolved fluorescence integrated from 525 to 545 nm of a solution-grown single crystal of tetracene at (a) 325, (b) 298, (c) 250, and (d) 200 K. The time-integrated spectra of the same crystal from 0 to 500 ps (black) and 10 to 20 ns (red) at (e) 325, (f) 298, (g) 250, and (h) 200 K.

wavelength-integrated fluorescence decays for a single crystal at four different temperatures: 325, 298, 250, and 200 K. Two aspects of the fluorescence signal change as the temperature is decreased. First, the rate of the initial singlet decay decreases, indicating that SF is slowing down. Analysis of the temperature dependence is complicated by the fact that the changes in fluorescence decay dynamics are accompanied by changes in the spectral shape. Figure 5e–h shows the prompt (0–100 ps) and delayed (10–20 ns) fluorescence spectra at the four temperatures. Ideally, the spectrum of the DF would mirror that of the prompt fluorescence, and this is indeed the case at 325 and 298 K. At 250 and 200 K, however, it appears that the true delayed fluorescence is now accompanied by a new red-shifted emitting species. Below 200 K, crystalline tetracene can undergo at least one solid-state phase transition[59−61] that can lead to changes in fluorescence. The origin of the low-energy emitting species at 200 K is not clear. The large red-shift and lack of vibronic structure suggests an excimer-like species, but crystalline tetracene can support a large variety of emissive defects,[62] and assignment of the temperature-dependent emission spectra is reserved for future work. The complicated spectral behavior is mirrored by a complex temperature dependence of the prompt fluorescence decay. Although the data in Figure 5 are suggestive of a simple Arrhenius behavior for k_{1n}, we found that the single-crystal decay of the high-energy singlet peak becomes more rapid at 77 K, similar to what we have observed in polycrystalline films.[42] Figure S3 of the Supporting Information plots the temperature dependence of the prompt fluorescence decay rate, which is clearly non-Arrhenius over the entire temperature range. If we consider only the three highest temperature points, where the decrease of k_{1n} is approximately linear, we can estimate an activation energy of ~500 cm^{-1}. This value is less than the value of 1000–2000 cm^{-1} usually assumed for tetracene, but the very limited temperature range of our data makes it a very crude estimate. The important point is that, as we earlier concluded for tetracene thin films, the temperature-dependent photoluminescence cannot be understood simply in terms of a one species (i.e., the singlet exciton) that decays via a single relaxation channel (i.e., SF).

With these factors in mind, we will consider only the temperature range 325–200 K, well above the point where tetracene undergoes a solid-state phase transition, where it appears that the expected slowdown for SF as an activated process is occurring. As the SF rate decreases, the visibility of the oscillations decreases as well. In Figure 6a–d, we plot the oscillatory component of the signal from Figure 5a–d. The oscillations have completely disappeared by 200 K. In Figure 6e–h, we plot the calculated oscillations as the k_{1n} rates change

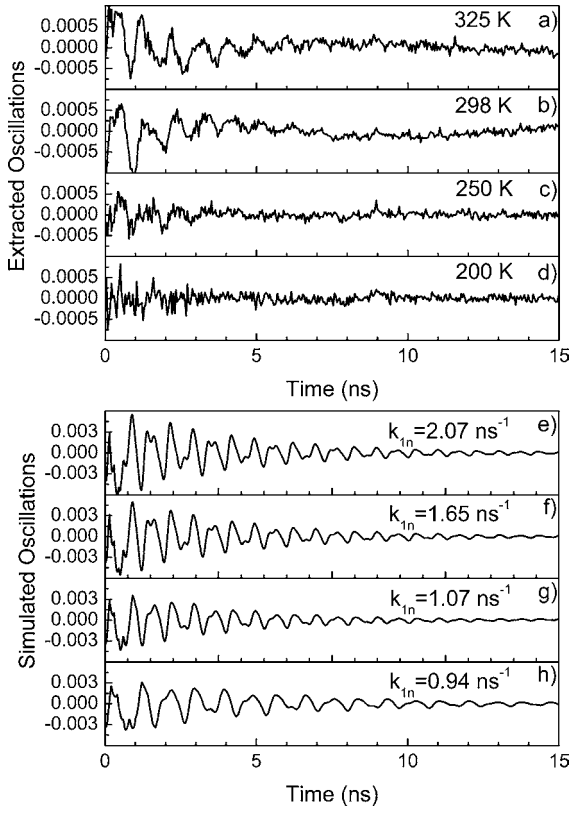

Figure 6. Extracted oscillations at (a) 325, (b) 298, (c) 250, and (d) 200 K. Simulated oscillations with the k_{1n} rate adjusted to match the fit of the experimental data for 325 K with (e) k_{1n} = 2.07 ns^{-1}, 298 K with (f) k_{1n} = 1.65 ns^{-1}, 250 K with (g) k_{1n} = 1.07 ns^{-1}, and 200 K with (h) k_{1n} = 0.94 ns^{-1}. The other values for the simulation are k_{n1} = 0.1 ns^{-1}, k_{rad} = 0.08 ns^{-1}, T_{2TT} = 10 ns, D^* = −0.186 ns^{-1}, and E^* = 0.744 ns^{-1}.

dx.doi.org/10.1021/ja301683w | J. Am. Chem. Soc. 2012, 134, 8597–8607

from 2.07 ns^{-1} at 325 K to 0.94 ns^{-1} at 200 K, values that reflect the slowdown in the decay rate of the prompt fluorescence. This factor of 2 change in k_{1n} leads to roughly a factor of 2 decrease in the visibility of the simulated oscillations. The relative FT amplitudes are much less sensitive to small changes in the k_{1n} rates and do not change. Both experimental and simulated data show the same trend, smaller oscillations as k_{1n} decreases, but the effect is much more pronounced in the experimental data. We suspect that the replacement of the DF signal by the lower energy emission at 200 K may play a role in decreasing the overall amount of DF and thus the visibility of the oscillations. The combination of a slower SF rate and competition from lower energy trap states may explain the almost total loss of oscillations at 200 K.

5. Magnetic Dipole−Dipole Coupling between Triplet Excitons. In the preceding analysis, we have assumed that the triplet−triplet interaction was negligible and that the triplet pair energies correspond to twice those of the zero-field Hamiltonian for a single triplet exciton. If the interaction term is nonnegligible, then we would expect to see shifts in the energies and in the singlet character of the stationary triplet pair states. For two interacting triplet excitons denoted A and B, we can follow the treatment of Benk and Sixl[63] and write

$$\hat{H}_{tot} = \hat{H}^{A}_{zero} + \hat{H}^{B}_{zero} + \hat{H}^{AB}_{int} \quad (12)$$

In the simplest limit of parallel magnetic dipoles interacting via dipole−dipole coupling,

$$\hat{H}^{AB}_{int} = X\hat{S}^{A}_{x}\hat{S}^{B}_{x} + XA\hat{S}^{A}_{y}\hat{S}^{B}_{y} - X(1+A)\hat{S}^{A}_{z}\hat{S}^{B}_{z} + X\alpha(\hat{S}^{A}_{z}\hat{S}^{B}_{y} + \hat{S}^{A}_{y}\hat{S}^{B}_{z}) \quad (13)$$

where

$$X = \frac{g^2\mu_B^2}{R_{AB}^3} \quad (14a)$$

$$A = 1 - 3\sin(\varphi)^2 \quad (14b)$$

$$\alpha = \sqrt{(1-A)(2+A)} \quad (14c)$$

In these equations, the EPR g-factor $g = 2.002$, $\mu_B = 9.274 \times 10^{-24}$ J/T is the Bohr magneton, and ϕ is the angle of the magnetic z-axis with respect to the intermolecular distance vector $\vec{R}_{AB}$. For $R_{AB} = 5.125$ Å, the distance between nearest neighboring tetracenes in the crystal,[64] we find that $X = 0.013$ cm^{-1}, comparable to the zero-field splitting energies. If the triplets are created within close proximity to each other, as would be expected in SF, then it is possible that their interaction could lead to shifts in energies and spin state coefficients. A complete analysis of the interactions between triplet excitons is beyond the scope of this paper. Here we give a simple example of how magnetic dipole−dipole interactions could affect the oscillations observed in the DF. We consider the case of two triplets whose z-axis magnetic tensors are parallel and aligned along the $\vec{R}_{AB}$ separation vector ($\phi = 0$). Since the z^* axis in crystalline tetracene is aligned close to the crystal b-axis,[24] this situation is not physically unreasonable for a pair of triplets trapped in the ab plane. Here we will only consider the effect of $\hat{H}^{AB}_{int}$ on the observed oscillation frequencies, since these quantities have been measured to greater precision than the relative FT amplitudes. By diagonalizing $\hat{H}_{tot}$ in the zero-field product basis for various values of X, we can find the energies of the three triplet pair states with singlet character and calculate their beat frequencies in the DF signal. As X increases, these states shift farther apart and the frequencies of all three oscillations increase, as shown in Figure 7. Even given the uncertainty range in the frequencies

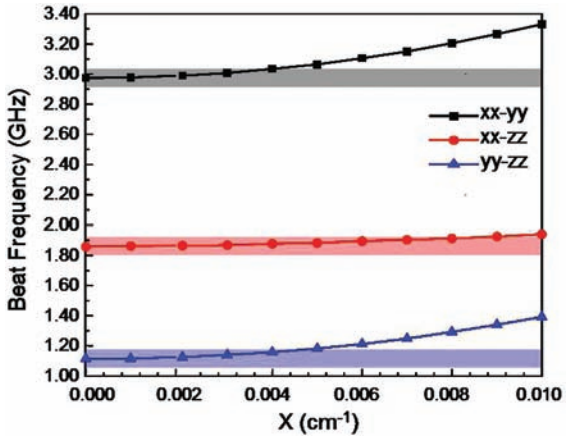

Figure 7. The transparent boxes indicate the experimental error in the beat frequencies and also reflect the error in the zero-field parameters from ref 24. The lines represent the calculated energy splittings of the triplet pair states with singlet character as X, the strength of the magnetic dipole−dipole interaction between triplet excitons, is increased.

as discussed above, the data in Figure 7 allow us to make a conservative estimate for the upper limit of $X \leq 0.006$ cm^{-1}. Using eq 14a, we would estimate that the triplets must be at least 6.5 Å apart. If we assume that the small X value reflects a large R_{AB} value, it is interesting to speculate as to why the distance between the two triplets would be greater than the nearest neighbor spacing. One explanation is that this separation arises from the delocalized nature of the initial singlet exciton,[55,65,66] which allows triplets to be created at larger separations than would be expected for a singlet state localized on only one molecule. Instead of being created on nearest neighbor tetracene molecules, the delocalized singlet could spawn triplets on opposite sides of a 3 × 3 array of tetracene molecules with a separation $R_{AB} > 1$ nm. A second mechanism that could generate large separations is rapid spatial diffusion of the triplets. Estimates for the diffusion constant of a triplet exciton in crystalline tetracene vary,[67−71] but even a low value of 10^{-5} cm^2/s could increase their separation by a nanometer or more within the first nanosecond. The surprising thing about such an explanation is that this would require that spin coherence is maintained while the triplets randomly jump between sites in the crystal. Finally, we should emphasize that we have assumed $\phi = 0$ and that the triplets are stationary. If these assumptions are relaxed, then there may be alternative explanations for the lack of an observable effect from magnetic dipole−dipole interactions. For example, rather than a large R_{AB}, it is possible that rapid reorientation of the triplets could average the dipole−dipole interaction term to zero, in much the same way that rapid reorientation washes out the effects of magnetic dipolar effects in NMR spectroscopy.[72] In the analysis of tetracene's EPR spectroscopy, it is assumed that the triplets are hopping back and forth between molecules on a time scale rapid compared with the EPR time scale, so that the crystal field parameters actually reflect an average of the nonequivalent crystallographic sites.[24,73] Rapid changes in ϕ or other orientation angles could average the $\hat{H}^{AB}_{int}$ term to zero, although

dx.doi.org/10.1021/ja301683w | J. Am. Chem. Soc. 2012, 134, 8597−8607

more detailed modeling is required in order to prove that this is actually the case.

6. Relation of Results to Previous Work and Mechanism of SF. We now try to place our results on the DF quantum beats into context with previous work by our group and others on the photophysics of crystalline tetracene. The density matrix model presented in this paper is based on the "direct" mechanism of SF, where the transition to the triplet manifold directly creates a triplet pair superposition state. It should be noted, however, that the observation of the spin signature of triplet superposition states in the DF does not necessarily rule out a charge-transfer intermediate, since this observation requires only that spin coherence is preserved throughout the SF process. Spin-conserving electron transfer processes are routinely observed in condensed phase systems,[74−76] and it is possible that two sequential electron transfer events (as in the "indirect" mechanism) could maintain spin coherence as well. If this was the case, however, the intermediate charge-transfer state must be relatively short-lived, since our modeling shows that the initial singlet decay is sufficient to explain the relative oscillation amplitudes and visibility. Detailed simulations of our data using a more complicated model with one or more intermediate states would allow us to place quantitative limits on the lifetime of such an intermediate, but in the absence of constraints for such a model, we elected not to explore this possibility computationally. Based on the good agreement between the data and our simple model, we surmise that the triplet pair superposition state is formed as a result of a direct transition from the initially excited singlet. Later, after this superposition state is dephased, two free triplet excitons are formed.

In addition to the mechanism of SF, we also need to consider the rate of this process. We were surprised to find such a large difference (more than a factor of 2) between the prompt singlet decay rates in polycrystalline versus single-crystal samples. The very low optical density of our solution-grown crystals helps rule out effects like reabsorption−re-emission events as an explanation for the longer decay in these samples. One possible explanation is that SF is actually more rapid in the films due to their disorder, which could lead to configurations (e.g., face-to-face) that are more favorable for SF.[10] A second explanation is that there is some other singlet decay channel in addition to SF in the films that is not present in the crystals. But it is important to note that the quantum beating that is a signature of the formation of triplet pair states via SF is present in both types of samples. Equations 10 allow us to make a rough estimate of the electronic coupling between the triplet pair state and the singlet. If we take the electronic dephasing time T_{2TS} to be 100 fs, a typical value for condensed phase systems, and use k_{1n} = 1.65 ns^{-1}, we find that M_{1n} is on the order of 5 cm^{-1}. This value is less than the width of the absorption spectrum, and consequently the weak coupling between the two states would not result in any noticeable splittings or intensity redistribution in the linear spectroscopy. This estimate of M_{1n} is also a least 2 orders of magnitude smaller than that deduced for pentacene,[50] a system that undergoes much more rapid SF.

Finally, we discuss the temperature dependence of the SF rate. In our earlier experiments on polycrystalline tetracene films, we found that a rapid decay of the J-type singlet exciton was present at 298, 77, and 4 K.[42,77] The ∼100 ps SF relaxation channel that is presumed to dominate at room temperature did not appear to be thermally activated, despite the fact that the DF disappeared as the temperature was lowered. We concluded that SF did not appear to be thermally activated, but this conclusion may need to be revised in light of the data in Figures 5 and 6 and Figure S3, Supporting Information. In the limited temperature range 325−200 K, the singlet decay does slow down at lower temperatures, although the decay speeds up again at even lower temperatures. Previously, we had postulated that the persistent 100 ps decay could reflect a barrierless relaxation channel into a dark intermediate whose subsequent dissociation into free triplets was thermally activated. But if we assign the dark state to a triplet pair superposition, this state would have to be lower in energy by hundreds of cm^{-1} relative to that of two free triplet excitons in order to provide a barrierless transition from the singlet. Such a lowering of the energy would imply that the two excitons have strong electronic interactions, and it is not clear whether such a bound pair would also exhibit spin properties similar to those of unperturbed triplets, as found in this work. One would have to assume that the electronic wave function of such a state is effectively decoupled from its spin properties, an assertion that can only be tested by further experiments or by computation. The temperature dependence of the singlet exciton decay in both polycrystalline tetracene films and single crystals continues to be somewhat of a puzzle. The one thing that we can say is that our results are not consistent with a simple single channel SF process that is thermally activated, as assumed by most previous workers.

■ CONCLUSIONS

In this work, we have revisited the earlier results by Chabr et al. where quantum beats from coherent triplet pairs were first observed. We have examined how these oscillations depend on sample morphology, temperature, and excitation energy. A density matrix model for this process has been developed that can quantitatively describe the frequencies, amplitudes, and damping of the oscillations. The damping of the oscillations on the 20 ns time scale is driven partly by population exchange between triplet and singlet manifolds and does not necessarily reflect the pure dephasing rates of the triplet pair states. The decrease in oscillation visibility at lower temperatures is consistent with the observed slowdown in the SF rate, but the effect is much stronger in the experiments than in the simulated data. Analysis of the quantum beat frequencies provides no indication that triplet−triplet interactions are important on the nanosecond time scale in the coherent triplet pairs. This work provides strong evidence for the direct, incoherent production of triplet pair superposition states with overall singlet character, as predicted by earlier kinetic theories of SF. While it does not answer all questions about the process, in particular the precise electronic structure of the triplet superposition state that lives for ∼10 ns after SF, it does clarify issues concerning the overall rate and nature of the product state. Further experiments to study the effects of magnetic fields and crystal morphology on the dynamics of SF are currently underway in our laboratory.

■ ASSOCIATED CONTENT

Ⓢ Supporting Information

Details of the single-crystal absorption spectrometer, single-crystal characterization, and the full derivation of the density matrix theory. This material is available free of charge via the Internet at http://pubs.acs.org.

AUTHOR INFORMATION

Corresponding Author

christopher.bardeen@ucr.edu

Notes

The authors declare no competing financial interest.

ACKNOWLEDGMENTS

This research was supported by the National Science Foundation, Grant DMR-0907310. Fluorescence lifetime measurements were performed on an instrument purchased with support from the National Science Foundation, Grant CRIF-0840055.

REFERENCES

(1) Hanna, M. C.; Nozik, A. J. *J. Appl. Phys.* **2006**, *100*, No. 074510.
(2) Shpaisman, H.; Niitsoo, O.; Lubomirsky, I.; Cahen, D. *Sol. Energy Mater. Sol. Cells* **2008**, *92*, 1541.
(3) Nozik, A. J. *Physica E* **2002**, *14*, 115.
(4) Schaller, R. D.; Klimov, V. I. *Phys. Rev. Lett.* **2004**, *92*, No. 186601.
(5) Sambur, J. B.; Novet, T.; Parkinson, B. A. *Science* **2010**, *330*, 63.
(6) Semonin, O. E.; Luther, J. M.; Choi, S.; Chen, H. Y.; Gao, J.; Nozik, A. J.; Beard, M. C. *Science* **2011**, *334*, 1530.
(7) Gabor, N. M.; Zhong, Z.; Bosnick, K.; Park, J.; McEuen, P. L. *Science* **2009**, *325*, 1367.
(8) Wang, S.; Khafizov, M.; Tu, X.; Zheng, M.; Krauss, T. D. *Nano Lett.* **2010**, *10*, 2381.
(9) Singh, S.; Jones, W. J.; Siebrand, W.; Stoicheff, B. P.; Schneider, W. G. *J. Chem. Phys.* **1965**, *42*, 330.
(10) Smith, M. B.; Michl, J. *Chem. Rev.* **2010**, *110*, 6891.
(11) Paci, I.; Johnson, J. C.; Chen, X.; Rana, G.; Popovic, D.; David, D. E.; Nozik, A. J.; Ratner, M. A.; Michl, J. *J. Am. Chem. Soc.* **2006**, *128*, 16546.
(12) Wang, C.; Tauber, M. J. *J. Am. Chem. Soc.* **2010**, *132*, 13988.
(13) Johnson, J. C.; Nozik, A. J.; Michl, J. *J. Am. Chem. Soc.* **2010**, *132*, 16302.
(14) Wilson, M. W. B.; Rao, A.; Clark, J.; Kumar, R. S. S.; Brida, D.; Cerullo, G.; Friend, R. H. *J. Am. Chem. Soc.* **2011**, *133*, 11830.
(15) Ryasnyanskiy, A.; Biaggio, I. *Phys. Rev. B* **2011**, *84*, No. 193203.
(16) Muller, A. M.; Avlasevich, Y. S.; Mullen, K.; Bardeen, C. J. *Chem. Phys. Lett.* **2006**, *421*, 518.
(17) Muller, A. M.; Avlasevich, Y. S.; Schoeller, W. W.; Mullen, K.; Bardeen, C. J. *J. Am. Chem. Soc.* **2007**, *129*, 14240.
(18) Michl, J.; Nozik, A. J.; Chen, X.; Johnson, J. C.; Rana, G.; Akdag, A.; Schwerin, A. F. *Proc. SPIE* **2007**, *6656*, No. 66560E.
(19) Greyson, E. C.; Stepp, B. R.; Chen, X.; Schwerin, A. F.; Paci, I.; Smith, M. B.; Akdag, A.; Johnson, J. C.; Nozik, A. J.; Michl, J.; Ratner, M. A. *J. Phys. Chem. B* **2010**, *114*, 14223.
(20) Greyson, E. C.; Vura-Weis, J.; Michl, J.; Ratner, M. A. *J. Phys. Chem. B* **2010**, *114*, 14168.
(21) Zimmerman, P. M.; Zhang, Z.; Musgrave, C. B. *Nat. Chem.* **2010**, *2*, 648.
(22) Zimmerman, P. M.; Bell, F.; Casanova, D.; Head-Gordon, M. *J. Am. Chem. Soc.* **2011**, *133*, 19944.
(23) Swenberg, C. E.; Stacy, W. T. *Chem. Phys. Lett.* **1968**, *2*, 327.
(24) Yarmus, L.; Rosenthal, J.; Chopp, M. *Chem. Phys. Lett.* **1972**, *16*, 477.
(25) Swenberg, C. E.; Metter, R. V.; Ratner, M. *Chem. Phys. Lett.* **1972**, *16*, 482.
(26) Frankevich, E. L.; Lesin, V. I.; Pristupa, A. I. *Chem. Phys. Lett.* **1978**, *58*, 127.
(27) Barhoumi, T.; Monge, J. L.; Mejatty, M.; Bouchriha, H. *Eur. Phys. J. B* **2007**, *59*, 167.
(28) Geacintov, N.; Pope, M.; Vogel, F. *Phys. Rev. Lett.* **1969**, *22*, 593.
(29) Merrifield, R. E.; Avakian, P.; Groff, R. P. *Chem. Phys. Lett.* **1969**, *3*, 155.
(30) Bouchriha, H.; Ern, V.; Fave, J. L.; Guthmann, C.; Schott, M. *J. Phys. (Paris)* **1978**, *39*, 257.
(31) Jadhav, P. J.; Mohanty, A.; Sussman, J.; Lee, J.; Baldo, M. A. *Nano Lett.* **2011**, *11*, 1495.
(32) Jundt, C.; Klein, G.; Sipp, B.; Moigne, J. L.; Joucla, M.; Villaeys, A. A. *Chem. Phys. Lett.* **1995**, *241*, 84.
(33) Marciniak, H.; Fiebig, M.; Huth, M.; Schiefer, S.; Nickel, B.; Selmaier, F.; Lochbrunner, S. *Phys. Rev. Lett.* **2007**, *99*, No. 176402.
(34) Thorsmolle, V. K.; Averitt, R. D.; Demsar, J.; Smith, D. L.; Tretiak, S.; Martin, R. L.; Chi, X.; Crone, B. K.; Ramirez, A. P.; Taylor, A. J. *Phys. Rev. Lett.* **2009**, *102*, No. 017401.
(35) Rao, A.; Wilson, M. W. B.; Hodgkiss, J. M.; Albert-Seifried, S.; Bassler, H.; Friend, R. H. *J. Am. Chem. Soc.* **2010**, *132*, 12698.
(36) Grumstrup, E. M.; Johnson, J. C.; Damrauer, N. H. *Phys. Rev. Lett.* **2010**, *105*, No. 257403.
(37) Frolov, S. V.; Kloc, C.; Schon, J. H.; Batlogg, B. *Chem. Phys. Lett.* **2001**, *334*, 65.
(38) Marciniak, H.; Pugliesi, I.; Nickel, B.; Lochbrunner, S. *Phys. Rev. B* **2009**, *79*, No. 235318.
(39) Rao, A.; Wilson, M. W. B.; Albert-Seifried, S.; Pietro, R. D.; Friend, R. H. *Phys. Rev. B* **2011**, *84*, No. 195411.
(40) Chabr, M.; Wild, U. P.; Funfschilling, J.; Zschokke-Granacher, I. *Chem. Phys.* **1981**, *57*, 425.
(41) Funfschilling, J.; Zschokke-Granacher, I.; Canonica, S.; Wild, U. P. *Helv. Phys. Acta* **1985**, *58*, 347.
(42) Burdett, J. J.; Gosztola, D.; Bardeen, C. J. *J. Chem. Phys.* **2011**, *135*, No. 214508.
(43) Campillo, A. J.; Hyer, R. C.; Shapiro, S. L.; Swenberg, C. E. *Chem. Phys. Lett.* **1977**, *48*, 495.
(44) Fleming, G. R.; Millar, D. P.; Morris, G. C.; Morris, J. M.; Robinson, G. W. *Aust. J. Chem.* **1977**, *30*, 2353.
(45) McGlynn, S. P. *Molecular Spectroscopy of the Triplet State*; Prentice-Hall: Englewood Cliffs, NJ, 1969.
(46) Merrifield, R. E. *J. Chem. Phys.* **1968**, *48*, 4318.
(47) Swenberg, C. E.; Geacintov, N. E. In *Organic Molecular Photophysics*; Birks, J. B., Ed.; Wiley & Sons: Bristol, U.K., 1973; Vol. *1*, p 489.
(48) Casperson, L. W. *Phys. Rev. A* **1997**, *55*, 3073.
(49) Bardeen, C. J.; Cao, J.; Brown, F. L. H.; Wilson, K. R. *Chem. Phys. Lett.* **1999**, *302*, 405.
(50) Chan, W. L.; Ligges, M.; Jailaubekov, A.; Kaake, L.; Miaja-Avila, L.; Zhu, X. Y. *Science* **2011**, *334*, 1541.
(51) Schmidt, J.; van der Waals, J. H. In *Time Domain Electron Spin Resonance*; Kevan, L., Schwartz, R. N., Eds.; Wiley: New York, 1979.
(52) *Chemically Induced Magnetic Polarization*; Lepley, A. R., Closs, G. L., Eds.; Wiley: New York, 1973.
(53) Kobori, Y.; Fuki, M.; Murai, H. *J. Phys. Chem. B* **2010**, *114*, 14621.
(54) Kothe, G.; Yago, T.; Weidner, J. U.; Link, G.; Lukaschek, M.; Lin, T. S. *J. Phys. Chem. B* **2010**, *114*, 14755.
(55) Lim, S. H.; Bjorklund, T. G.; Spano, F. C.; Bardeen, C. J. *Phys. Rev. Lett.* **2004**, *92*, No. 107402.
(56) Arnold, S.; Alfano, R. R.; Pope, M.; Yu, W.; Ho, P.; Selsby, R.; Tharrats, J.; Swenberg, C. E. *J. Chem. Phys.* **1976**, *64*, 5104.
(57) Smith, A. W.; Weiss, C. *Chem. Phys. Lett.* **1972**, *14*, 507.
(58) Lopez-Delgado, R.; Miehe, J. A.; Sipp, B. *Opt. Commun.* **1976**, *19*, 79.
(59) Jankowiak, R.; Kalinowski, J.; Konys, M.; Buchert, J. *Chem. Phys. Lett.* **1979**, *65*, 549.
(60) Sondermann, U.; Kutoglu, A.; Bassler, H. *J. Phys. Chem.* **1985**, *89*, 1735.
(61) Venuti, E.; Valle, R. G. D.; Farina, L.; Brillante, A.; Masino, M.; Girlando, A. *Phys. Rev. B* **2004**, *70*, No. 104106.
(62) Piryatinskii, Y. P.; Kurik, M. V. *Mol. Mater.* **1992**, *1*, 43.
(63) Benk, H.; Sixl, H. *Mol. Phys.* **1981**, *42*, 779.
(64) Holmes, D.; Kumaraswamy, S.; Matzger, A. J.; Vollhardt, K. P. C. *Chem.—Eur. J.* **1999**, *5*, 3399.
(65) Voigt, M.; Langner, A.; Schouwink, P.; Lupton, J. M.; Mahrt, R. F.; Sokolowski, M. *J. Chem. Phys.* **2007**, *127*, No. 114705.

(66) Camposeo, A.; Polo, M.; Tavazzi, S.; Silvestri, L.; Spearman, P.; Cingolani, R.; Pisignano, D. *Phys. Rev. B* **2010**, *81*, No. 033306.
(67) Vaubel, G.; Kallmann, H. *Phys. Status Solidi* **1969**, *35*, 789.
(68) Pope, M.; Geacintov, N. E.; Saperstein, D.; Vogel, F. *J. Luminesc.* **1970**, *1* (2), 224.
(69) Kalinowski, J. *J. Luminesc.* **1976**, *11*, 393.
(70) Aladekomo, J. B.; Arnold, S.; Pope, M. *Phys. Status Solidi B* **1977**, *80*, 333.
(71) Bizzaro, W.; Yarmus, L.; Rosenthal, J.; Berk, N. F. *Phys. Rev. B* **1981**, *23*, 5673.
(72) Abragam, A. *Principles of Nuclear Magnetism*; Clarendon: Oxford, U.K., 1961.
(73) Sternlicht, H.; McConnell, H. M. *J. Chem. Phys.* **1961**, *35*, 1793.
(74) Verhoeven, J. W. *J. Photochem. Photobiol. C* **2006**, *7*, 40.
(75) Shaakov, S.; Galili, T.; Stavitski, E.; Levanon, H.; Lukas, A.; Wasielewski, M. R. *J. Am. Chem. Soc.* **2003**, *125*, 6563.
(76) Poluektov, O. G.; Paschenko, S. V.; Utschig, L. M. *Phys. Chem. Chem. Phys.* **2009**, *11*, 6750.
(77) Burdett, J. J.; Muller, A. M.; Gosztola, D.; Bardeen, C. J. *J. Chem. Phys.* **2010**, *133*, No. 144506.